

# Bypassing the energy functional in density functional theory: Direct calculation of electronic energies from conditional probability densities

Ryan J. McCarty,<sup>1</sup> Dennis Perchak,<sup>1</sup> Ryan Pederson,<sup>2</sup> Robert Evans,<sup>3</sup> Yiheng Qiu,<sup>2</sup> Steven R. White,<sup>2</sup> and Kieron Burke<sup>1, 2, \*</sup>

<sup>1</sup>*Department of Chemistry, University of California, Irvine, CA, 92697*

<sup>2</sup>*Department of Physics and Astronomy, University of California, Irvine, CA, 92697*

<sup>3</sup>*H H Wills Physics Laboratory, University of Bristol, Bristol BS8 1TL, UK*

(Dated: Tuesday 11<sup>th</sup> October, 2022)

Accurate ground-state energies are the focus of most electronic structure calculations, so density functional calculations often fail for want of an accurate exchange-correlation approximation. But the energy can instead be extracted from a sequence of density functional calculations of conditional probabilities (CP-DFT). Simple CP approximations yield usefully accurate results for a broad range of systems: two-electron ions, the hydrogen dimer, and the uniform gas at all temperatures. CP-DFT has no self-interaction error for one electron, and correctly dissociates H<sub>2</sub>, both major challenges in standard density functional theory. Orbital free CP-DFT may be ideal for warm dense matter simulations.

Modern electronic structure calculations usually focus on finding accurate ground-state energies, as many predicted properties of a molecule or a material depend on this ability [1]. Wavefunction-based methods, such as coupled-cluster theory [2, 3] or quantum Monte Carlo (QMC) [4, 5], directly yield energies. Kohn-Sham (KS) density functional theory (DFT) [6] incorporates the many-electron problem into the exchange-correlation (XC) energy, which must be approximated as a functional of spin densities. Hundreds of XC functionals with distinct approximations are available in standard codes [7], reflecting the tremendous difficulty in finding general, accurate approximations. Recently, KS-DFT at finite temperatures, based on the Mermin theorem [8], has been tremendously successful in simulations of warm dense matter [9, 10].

We propose an alternative to KS-DFT, in which we directly calculate conditional probability densities, from which the energy can be calculated. This bypasses all the difficulties of approximating the XC energy. The electronic pair density can always be written as

$$P(\mathbf{r}, \mathbf{r}') = n(\mathbf{r}) \tilde{n}_{\mathbf{r}}(\mathbf{r}'), \quad (1)$$

where  $n(\mathbf{r})$  is the single particle density, and  $\tilde{n}_{\mathbf{r}}(\mathbf{r}')$  is the conditional probability (CP) density of finding an electron at  $\mathbf{r}'$ , given an electron at  $\mathbf{r}$ . The standard exact KS potential of DFT,  $v_s[n](\mathbf{r})$ , is defined to yield  $n(\mathbf{r})$  in an effective fermionic non-interacting problem [11]. A conditional probability KS potential (CPKS),  $v_s[\tilde{n}_{\mathbf{r}}](\mathbf{r}')$  yields  $\tilde{n}_{\mathbf{r}}(\mathbf{r}')$  from such a KS calculation with  $N - 1$  electrons. Because standard KS-DFT calculations usually yield highly accurate densities [12], an accurate CPKS potential should yield highly accurate XC energies. Unlike XC approximations built on theories of the XC hole [13], here we *calculate* that hole.

Just as in traditional DFT, we construct a simple, universal approximation for the CP KS potential from exact conditions and the uniform gas. At large separations or high temperatures, the CP potential reduces to adding

$1/|\mathbf{r} - \mathbf{r}'|$  to the external potential, as if the missing electron were classical. We call this a blue electron (i.e. distinguishable from all others), recalling the Percus test particle of classical statistical mechanics [14]. However, at small separations, the electron-electron cusp condition [15], requires adding only 1/2 this potential (the 2 is due to the reduced mass). We locally interpolate between these two universal limits. Representative results are shown in Fig 1.

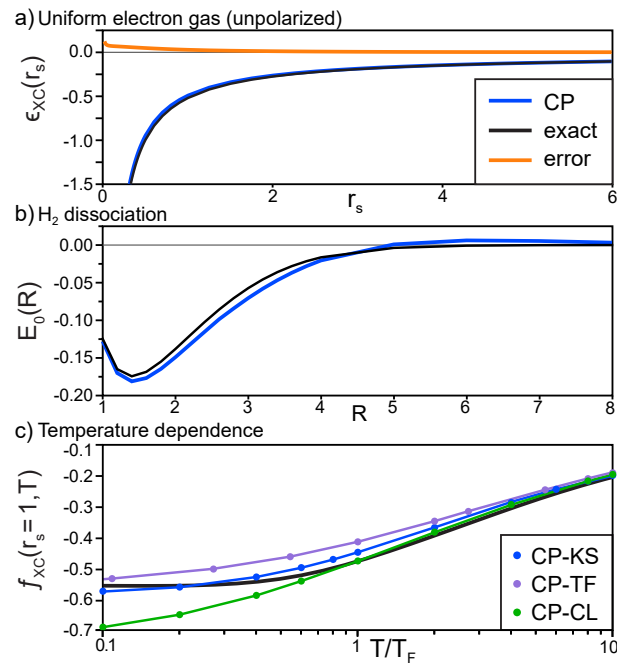


FIG. 1. CP (blue) and exact (black) energies: (a) XC energy per particle in uniform gas at increasing Wigner-Seitz radii ( $r_s$ ) and  $T = 0$ , (b) binding energy curve for H<sub>2</sub>, and (c) XC free energy per particle at  $r_s = 1$  as a function of reduced temperature ( $T_F$  is the Fermi temperature) for three different approximations: KS (Kohn-Sham), TF (Thomas-Fermi), and CL (classical)). Exact from Ref. [16] in (a), Ref. [17] in (c). Hartree atomic units used throughout.

For the uniform electron gas at zero temperature, our CP potential interpolation is extremely accurate. We added a strong repulsion for  $r_s < 1$ , to recover the exchange limit. The middle panel shows the  $H_2$  binding curve, where the inclusion of the electron-electron cusp is vital. Unlike semi-local DFT, CP-DFT dissociates the molecule correctly, remaining spin-unpolarized throughout. The bottom panel (c) shows that CP can be used at all temperatures  $T$ . As  $T$  is raised from very low to very high, the CP-DFT error never exceeds 20% and vanishes in the high temperature limit. Moreover, results of orbital-free Thomas-Fermi, and even classical, CP calculations agree reasonably with both KS-CP and the accurate results for all  $T > T_F$ .

**Theory:** We consider non-relativistic purely electronic problems, and use Hartree atomic units throughout. The pair density of the exact ground-state wavefunction  $\Psi^\lambda$ :

$$P^\lambda(\mathbf{r}_1, \mathbf{r}_2) = N(N-1) \sum_{\sigma_1 \sigma_2} \int d3 \dots dN |\Psi^\lambda(1 \dots N)|^2, \quad (2)$$

where  $N$  is the number of electrons. Here 1 denotes both  $\mathbf{r}_1$  and  $\sigma_1$ , the spatial and spin indices. The  $\lambda$ -dependence is the coupling constant in KS DFT, where the repulsion is multiplied by  $\lambda$  but the one-body potential  $v^\lambda(\mathbf{r})$  is adjusted to keep the ground-state density  $n(\mathbf{r})$  fixed [18]. The XC energy is:

$$E_{\text{XC}} = \frac{1}{2} \int_0^1 d\lambda \int d^3r \int d^3r' \frac{n(\mathbf{r}) [\tilde{n}_\mathbf{r}^\lambda(\mathbf{r}') - n(\mathbf{r})]}{|\mathbf{r} - \mathbf{r}'|}, \quad (3)$$

with  $\tilde{n}_\mathbf{r}^\lambda(\mathbf{r}') - n(\mathbf{r})$  being the  $\lambda$ -dependent XC hole, defined via the  $\lambda$ -dependent generalization of Eq. 1. Setting  $\lambda = 1$  in Eq. 3 yields  $U_{\text{XC}}$ , the potential contribution to XC. The integral over  $\lambda$  is called the adiabatic connection.

Denote  $v^\lambda[n](\mathbf{r})$  as the one body potential that yields the unique ground-state density for electron repulsion  $\lambda/|\mathbf{r} - \mathbf{r}'|$ . The conditional probability potential is

$$\tilde{v}^\lambda(\mathbf{r}'|\mathbf{r}) = v[\tilde{n}_\mathbf{r}^\lambda](\mathbf{r}') = v^\lambda[n](\mathbf{r}') + \Delta\tilde{v}_\mathbf{r}^\lambda[n](\mathbf{r}'), \quad (4)$$

being the unique potential whose ground-state density for Coulomb interacting electrons yields the exact  $\lambda$ -dependent CP density. The CP-KS potential is found self-consistently:

$$\tilde{v}_s^\lambda(\mathbf{r}'|\mathbf{r}) = v_s[\tilde{n}_\mathbf{r}^\lambda](\mathbf{r}') = \tilde{v}^\lambda(\mathbf{r}'|\mathbf{r}) + v_{\text{HXC}}[\tilde{n}_\mathbf{r}^\lambda](\mathbf{r}'), \quad (5)$$

where  $v_{\text{HXC}}$  is the Hartree-XC potential [1]. Thus knowledge of the CP correction potential,  $\Delta\tilde{v}_\mathbf{r}^\lambda[n](\mathbf{r}')$  in Eq. 4, allows a self-consistent KS calculation for the exact CP density. Uniqueness of the CP potential is guaranteed by the HK theorem. As  $\tilde{n}_\mathbf{r}^\lambda(\mathbf{r}')$  is non-negative, normalized to  $N-1$ , and found from a wavefunction, it is in the standard space of densities, for which we routinely assume KS potentials exist [19, 20].

The above equations are for pure density functionals, and their analogs for spin-density functionals are straightforward (but cumbersome). Decades of research in DFT can be

applied to the study of CP densities and potentials, yielding many exact conditions. For example, at  $\lambda = 0$  where the exchange hole is never positive,

$$\tilde{n}_\mathbf{r}^{\lambda=0}(\mathbf{r}') \leq n(\mathbf{r}'). \quad (6)$$

The CP densities satisfy a complementarity principle:

$$\tilde{n}_\mathbf{r}^\lambda(\mathbf{r}') = \frac{n(\mathbf{r}')}{n(\mathbf{r})} \tilde{n}_{\mathbf{r}'}^\lambda(\mathbf{r}), \quad (7)$$

which is Bayesian, and may be amenable to modern machine-learning methods. The electron coalescence cusp condition requires

$$\left. \frac{\partial \tilde{n}_\mathbf{r}^\lambda(\mathbf{r}, u)}{\partial u} \right|_{u=0} = \lambda \tilde{n}_\mathbf{r}^\lambda(\mathbf{r}), \quad (8)$$

where  $\mathbf{u} = \mathbf{r}' - \mathbf{r}$  and the left-hand side has been spherically averaged over  $\mathbf{r} + \mathbf{u}$  [21]. Using Ref. [22], write

$$\Psi^\lambda(1 \dots N) = \sqrt{\frac{n(\mathbf{r}_1)}{N}} \tilde{\Psi}_\mathbf{r}^\lambda(2 \dots N), \quad (9)$$

where  $\tilde{\Psi}_\mathbf{r}^\lambda$  is not antisymmetric under interchange of the electrons, but is uniquely defined by Eq. 9, and  $\tilde{n}_\mathbf{r}^\lambda$  is its density. For large  $r$ , Ref. [22] shows that  $\tilde{\Psi}_\mathbf{r}^\lambda$  becomes a ground-state of the  $N-1$  particle system and its gradients with respect to  $\mathbf{r}$  vanish, yielding

$$\Delta\tilde{v}_{\mathbf{r} \rightarrow \infty}^\lambda(\mathbf{r}') \rightarrow \frac{\lambda}{|\mathbf{r} - \mathbf{r}'|}, \quad (10)$$

i.e., the blue electron approximation becomes exact in this limit.

For  $N = 1$ ,  $\tilde{n}_\mathbf{r}^\lambda(\mathbf{r}') = 0$ , there is no self-interaction error [23]. If  $N = 2$ , the CP density has just one electron:

$$\tilde{\phi}_\mathbf{r}^\lambda(\mathbf{r}') = \sqrt{\tilde{n}_\mathbf{r}^\lambda(\mathbf{r}')} = \sqrt{\frac{2}{n(\mathbf{r})}} \Psi^\lambda(\mathbf{r}, \mathbf{r}'), \quad (11)$$

yielding

$$\tilde{v}_s^\lambda(\mathbf{r}'|\mathbf{r}) - \epsilon_\mathbf{r}^\lambda = \frac{1}{2} \frac{\nabla'^2 \Psi^\lambda(\mathbf{r}, \mathbf{r}')}{\Psi^\lambda(\mathbf{r}, \mathbf{r}')}, \quad (12)$$

where  $\epsilon_\mathbf{r}^\lambda$  is the eigenvalue of the CPKS potential. Because the wavefunction satisfies the Schrödinger equation, we find

$$\Delta\tilde{v}_s^\lambda(\mathbf{r}'|\mathbf{r}) + \Delta\tilde{v}_s^\lambda(\mathbf{r}|\mathbf{r}') = \frac{\lambda}{|\mathbf{r} - \mathbf{r}'|} - E^\lambda, \quad (13)$$

where  $\Delta\tilde{v}_s^\lambda(\mathbf{r}'|\mathbf{r}) = \tilde{v}_s^\lambda(\mathbf{r}'|\mathbf{r}) - v^\lambda[n](\mathbf{r}') - \epsilon_\mathbf{r}^\lambda$ .

**Approximations:** To perform a CP-DFT calculation, we need a general-purpose approximation to the CP potential,  $\Delta\tilde{v}_\mathbf{r}^\lambda(\mathbf{r}')$ . At large separations, the CP potential is simply  $\lambda/|\mathbf{r} - \mathbf{r}'|$  for all systems. At small separations, it is  $\lambda/(2|\mathbf{r} - \mathbf{r}'|)$ , to satisfy the electron-electron cusp condition,

for all systems. We interpolate between these two with a simple local density approximation

$$\Delta\tilde{v}_{\mathbf{r}}^{\lambda}[n](\mathbf{r}') \approx \frac{\lambda}{2|\mathbf{r} - \mathbf{r}'|} (1 + \text{Erf}\left(\frac{|\mathbf{r} - \mathbf{r}'|}{r_s(n(\mathbf{r}))}\right)), \quad (14)$$

where  $r_s = (3/(4\pi n))^{1/3}$  is the Wigner-Seitz radius at the reference point. We use this approximation for all ground-state CP calculations in the paper. Fig. 1 (a) and (b) use Eq. 14 combined with standard DFT approximations for  $v_{\text{XC}}$ . Fig. 1(c) uses simply  $\lambda/|\mathbf{r} - \mathbf{r}'|$ , as the difference is negligible at significant temperatures.

*Uniform electron gas:* The  $N$ -electron density is trivially a constant, and the one-body potential vanishes. The CP calculation is for  $N - 1$  electrons in a KS potential:

$$v_s(r) = \Delta\tilde{v}(r) + \int d^3r' \frac{\tilde{n}(\mathbf{r}') - n_0}{|\mathbf{r} - \mathbf{r}'|} + v_{\text{XC}}^{\text{LDA}}[\tilde{n}](\mathbf{r}), \quad (15)$$

where  $n_0 = N/V$  and

$$\Delta\tilde{v}(r) = \Delta\tilde{v}_0^{(\lambda=1)}(n_0, r) + A(r_s)e^{-r^2/2\sigma(r_s)^2}. \quad (16)$$

The second term is added to recover the correct high-density limit, i.e., the simple  $n^{4/3}$  exchange energy. If we run for many  $r_s$  values, we can perform the adiabatic connection integral by integrating over  $r_s$ , so we need only  $\lambda = 1$ . The XC potential is from [24]. The strength and range parameters of the added Gaussian potential are fitted to [24] for  $r_s = 0.02$ , where exchange dominates. The density is found self-consistently in a sphere using Fermi-surface smearing ( $T = 0.05T_F$ ). Imposing zero density flux through the surface of the sphere minimizes boundary effects. We find  $N = 512$  is sufficient for convergence. Further details will appear in a forthcoming paper.

Fig. 2 shows the hole density compared to that given by the parameterization of the uniform gas XC hole [25]. The agreement is very good, with the lowest accuracy from the on-top region, which has very little weight in the XC energy.

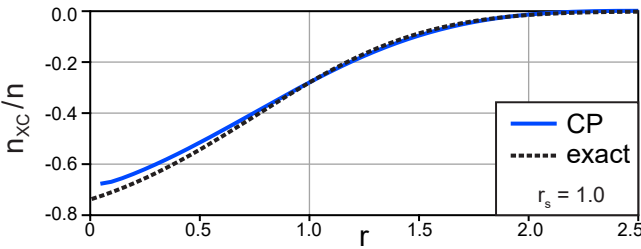


FIG. 2. Normalized XC hole densities for the uniform gas at  $r_s = 1$ , both CP (blue) and for the uniform electron gas [25] (black).

*Atoms and molecules:* We applied Eq. 14 to highly accurate calculations of 2-electron systems. These calculations were done using a new type of basis function called gausslets [26, 27] which are tailored for density matrix renormalization

group calculations [28] and based on wavelets. Gausslets resemble a variable-spaced real-space grid. The two-electron Hamiltonian terms have only two indices,  $V_{ij}$ , unlike the four indices needed in a standard basis. The grid-like structure make CP calculations easy to implement. A blue electron sitting at a point in space sits on a gausslet,  $i$ , located at its reference,  $\mathbf{r}_i$ . The repulsive one-electron potential at  $i$  is simply row  $i$  of  $V_{ij}$ , and integration likewise becomes point-wise sums. Recent innovations add a Gaussian basis to better describe atomic core behavior, further described in a forthcoming work. We used no more than 2000 gausslets with errors in total energies for  $Z = 1$  and  $Z = 2$  below 0.1 mH. To find the conditional probability using Eq. 14, we find the ground state of an  $N \times N$  matrix with the Lanczos algorithm [29] and repeat  $N$  times. Gausslets make an excellent basis for CP calculations, but in any basis, CP calculations are receptive to parallel computing, as each value of  $\mathbf{r}$  and  $\lambda$  can be computed independently.

In any CP calculation, one must first perform a standard DFT calculation that yields an accurate approximate density. For 2-electron ions presented in Table I, we choose Hartree-Fock, as it provides a bound density even for  $\text{H}^-$  [30]. We have performed the double integral over  $\mathbf{r}$  and  $\mathbf{r}'$  to find the potential contribution to correlation,  $U_c$ . The virial theorem for atoms (relating the total energy to total kinetic energy,  $E = -T$ ) then allows us to deduce  $E_c$ , without needing to perform the adiabatic connection. For He, the  $E_c$  error is just 6 mHa, and is only 22% for both  $U_c$  and  $E_c$ . As  $Z \rightarrow \infty$ , the CP calculation correctly yields a finite value. At the other end, for  $\text{H}^-$ , the error has increased to 10mH, but this anion is not even bound in a KS-DFT calculation with standard approximations [12].

$Z$	$E_{\text{X}}^{\text{HF}}$	$V_{\text{ee}}^{\text{CP}}$	$U_c^{\text{CP}}$	$U_c^{\text{Exact}}$	virial $E_c^{\text{CP}}$	$E_c^{\text{Exact}}$
1.0	-0.3959	0.2918	-0.1041	-0.0698	-0.0523	-0.0420
2.0	-1.0257	0.9301	-0.0956	-0.0786	-0.0479	-0.0421
3.0	-1.6516	1.5521	-0.0995	-0.0832	-0.0504	-0.0435
4.0	-2.2770	2.1750	-0.1020	-0.0857	-0.0525	-0.0443
6.0	-3.5273	3.4226	-0.1047	-0.0881	-0.0563	-0.0452

TABLE I. Results for 2-electron Helium-like ions using HF reference densities, where the virial  $E_c^{\text{CP}}$  is derived from the virial theorem for atoms.

The virial trick only works for Coulomb-interacting atoms and molecules at equilibrium. Otherwise, we need to perform the adiabatic connection integral. For  $N = 2$ , we know the exact result as  $\lambda \rightarrow 0$  (exchange limit), where  $\tilde{n}_{\mathbf{r}}^{\lambda=0}(\mathbf{r}') = n(\mathbf{r}')/2$ . By definition, for 2-electrons we have

$$\tilde{v}_s^{\lambda}(\mathbf{r}'|\mathbf{r}) = v_s[n](\mathbf{r}') - \lambda v_{\text{HX}}[n](\mathbf{r}') - v_c^{\lambda}[n](\mathbf{r}') + \Delta\tilde{v}_s^{\lambda}(\mathbf{r}'|\mathbf{r}). \quad (17)$$

In practice, obtaining  $v_c^{\lambda}[n](\mathbf{r}')$  is difficult, and we

approximate

$$\tilde{v}_s^\lambda(\mathbf{r}'|\mathbf{r}) \approx \begin{cases} v_s[n](\mathbf{r}'), \lambda = 0 \\ v[n](\mathbf{r}') + (1 - \lambda)v_{\text{HX}}[n](\mathbf{r}') + \Delta\tilde{v}_s^\lambda(\mathbf{r}'|\mathbf{r}) \end{cases} \quad (18)$$

to recover the exchange limit exactly. In the following calculation for  $\text{H}_2$ , we utilize the interpolated blue approximation, Eq. 14, for  $\Delta\tilde{v}_s^\lambda(\mathbf{r}'|\mathbf{r})$  and the exact density  $n(\mathbf{r}')$  throughout. We run for  $\lambda \in \{0.0, 0.1, 0.3, 0.5, 0.7, 1.0\}$ , and fit to a first-order Padé approximant, which is integrated analytically.

$R$	$E_x$	$V_{ee}^{\text{Blue}}$	$U_C^{\text{Blue}}$	$U_C^{\text{Exact}}$	$E_C^{\text{Blue}}$	$E_C^{\text{Exact}}$
1.0	-0.7472	0.6688	-0.0785	-0.0732	-0.0433	-0.0400
2.0	-0.5698	0.4720	-0.0978	-0.0835	-0.0587	-0.0478
4.0	-0.4323	0.2576	-0.1747	-0.1692	-0.1359	-0.1318
8.0	-0.3749	0.1241	-0.2497	-0.2499	-0.2445	-0.2477

TABLE II.  $\text{H}_2$  energies versus  $R$ , where  $E_C^{\text{Blue}}$  is computed from Eq. 18 with the exact density.

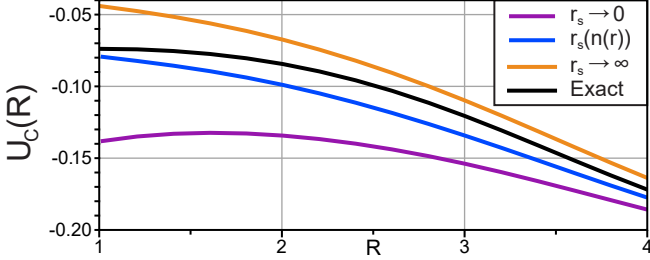


FIG. 3.  $U_C(R)$  from  $\text{H}_2$ . The pure blue electron approximation (purple), half that potential (orange), our interpolation, Eq. 14 using exact  $n(r)$  (blue), and exact (black). The interpolation error never exceeds 20%.

The binding curve for  $\text{H}_2$  as a function of bond length is shown in Fig 1(b), with components given in Table II. Fig. 3, shows  $U_C(R)$  for 3 distinct choices of CP potential. As  $R \rightarrow \infty$ , any version of the blue electron approximation becomes accurate. Consider what happens as the bond is stretched. The exact wavefunction has Heitler-London [31] form:

$$\Psi^\lambda(\mathbf{r}_1, \mathbf{r}_2) = \frac{1}{\sqrt{2}} (\phi_A(\mathbf{r}_1) \phi_B(\mathbf{r}_2) + \phi_B(\mathbf{r}_1) \phi_A(\mathbf{r}_2)) \quad (19)$$

where  $\phi_A$  and  $\phi_B$  are atomic orbitals localized on each of the two protons. This yields a conditional density:

$$n_A^\lambda(\mathbf{r}') = n_B(\mathbf{r}'), \quad \mathbf{r} \text{ near } A \quad (20)$$

and vice versa, for all  $\lambda \neq 0$ . Thus the Coulomb energy of the pair density vanishes due to the lack of overlap, and each atomic region correctly yields a one-electron energy of

a separate hydrogen atom. CP-DFT is an exact theory for bond dissociation, unlike the on-top hole theory of Ref. [32].

Hooke's atom consists of two Coulomb repelling electrons in a harmonic potential of force constant  $k$  [33]. At  $k = 1/4$ , the density is known analytically, and at  $r = 0$ , the exact  $\tilde{v}_s^\lambda(\mathbf{r}'|\mathbf{r})$  is radial. In Fig. 4 we compare the blue electron approximation, our interpolation formula Eq. 14, and the exact CP potential and the resulting densities  $\tilde{n}_r^\lambda(r')$ . Note the accuracy of the blue approximation for large  $r'$ , and the cusps as  $r' \rightarrow r$  in the exact and approximate CP densities.

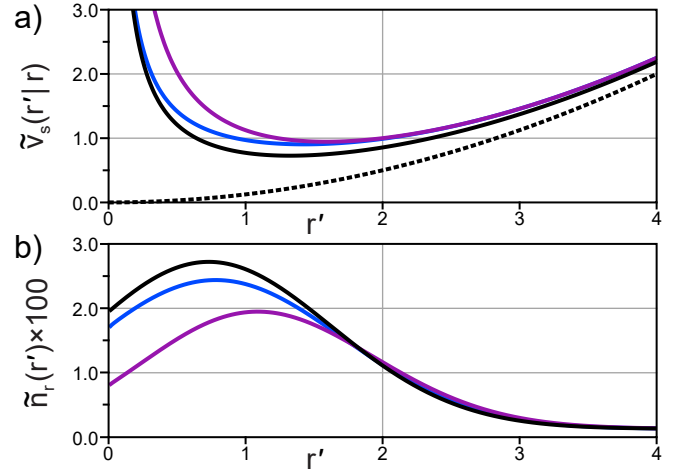


FIG. 4. Hooke's atom. Top:  $\tilde{v}_s(\mathbf{r}'|\mathbf{r})$  for the interpolation (Eq. 14, in blue), the pure blue electron (in purple), exact (in black), and the external potential  $r'^2/8$  (black dashed). Bottom:  $\tilde{n}_r(r')$  for the corresponding potentials.

In practical calculations, one does not have access to exact densities, but usually KS-DFT densities from standard approximations are accurate, and in many cases where they are not, Hartree-Fock densities are better[34]. In principle, if neither suffices, densities could be found self-consistently by minimizing the energy from CP calculations with respect to the  $N$ -electron density.

*Finite temperatures:* Possibly, the most important application of CP DFT is for thermal equilibrium in warm dense matter [9]. While thermal KS-DFT calculations have been very successful, finding consistent temperature-dependent approximations is more difficult than at zero temperature [35]. Moreover, calculations using KS solvers eventually fail at extremely high temperatures, due to convergence difficulties with orbital sums.

For finite temperatures, Eq 3 translates to  $F_{XC}$ , the XC contribution to the Helmholtz free energy, which folds in entropic contributions [8, 36]. To find accurate CP densities, we solve the KS equations with finite temperature occupations. (Thermal corrections to  $v_{xc}$  have been argued to have little effect on the orbitals [37]). In Fig. 1 (c), we showed results for the potential XC free energy at  $r_s = 1.0$  for a wide range of temperatures. The black curve displays the analytical parameterization (Ref. [17]). The KS CP approximation mildly overestimates  $f_{xc}$  for  $t = T/T_F$

between about 0.2 and 9, beyond which it fails to converge.

For higher temperatures, we performed a much simpler CP calculation using the Thomas-Fermi (TF) approximation [38, 39], often employed in warm dense matter [40, 41], and implementing the simple blue approximation. We first solved the TF equation at  $T = 0$ . This was used to initiate iterations for a full numerical solution. We make a simple interpolation of Perrot's [42] accurate parameterization of the Helmholtz free energy density  $f_0(n)$  of the uniform non-interacting electron gas constructed to yield the correct  $T = 0$  and (classical)  $T \rightarrow \infty$  limits:

$$f_0(n) = k_B T n \left( \ln(y) - c + a y^{\frac{2}{3}} \right), \quad (21)$$

where  $y = \pi^2 n / \sqrt{2} (k_B T)^{3/2}$ ,  $c = 1 - \ln(2/\sqrt{\pi})$ , and  $a = 9(2/3)^{1/3}/10$ . The Fermi temperature is given by  $k_B T_F = (3\pi^2 n)^{2/3}/2$ . As  $T \rightarrow 0$ ,  $f_0(n) = 3n k_B T_F / 5$  as required. TF theory corresponds to minimizing the Mermin [8] grand potential functional ignoring XC and making the local density approximation  $F[n] = \int d^3r f_0(n(r))$  for the non-interacting Helmholtz free energy.

*Classical connection:* In the classical limit TF theory reduces to the Poisson-Boltzmann (PB) theory used to treat electrical double layers and many other properties of electrolyte solutions and ionic liquids [43]. In the high temperature limit we can ignore the third term in Eq 21 yielding

$$F[n] = k_B T \int d^3r n(\mathbf{r}) \left( \ln \left( \frac{n(\mathbf{r}) \lambda^3}{2} \right) - 1 \right), \quad (22)$$

where  $\lambda = (2\pi/k_B T)^{1/2}$  is the thermal de Broglie wavelength. Eq. 22 is identical to the Helmholtz free energy functional of the ideal classical gas, apart from the residual spin degeneracy factor  $(2s+1)$ . Employing Eq. 22 from the outset corresponds to implementing the classical DFT [43, 44] that generates PB theory for the one-component plasma. In the classical limit the TF screening length,  $\lambda_{TF}$  [45], reduces to the Debye length  $\lambda_D$  of the OCP, given by  $(\lambda_D)^{-2} = 4\pi e^2 n / k_B T$ .

In Fig. 5 we show relative errors as a function of  $t = T/T_F$  over a larger temperature range than Fig. 1 (c). The blue KS approximation (blue curve) performs well across the range. Blue TF (purple curve) overestimates the XC free energy up to  $t \approx 10$ ; for larger values, all results merge. The classical approximation (green curve) becomes exact at sufficiently high  $t$ .

In the classical limit (Boltzmann statistics) the CP approach is equivalent to the Percus test particle procedure [14, 46]. Fixing a (classical) particle at the origin constitutes an external potential for the others. The resulting one-body density is proportional to the pair correlation function of the liquid[47]. The Percus procedure for quantum systems was pioneered by Chihara [46] and the most successful applications relate to liquid metals and electron-ion correlations[48].

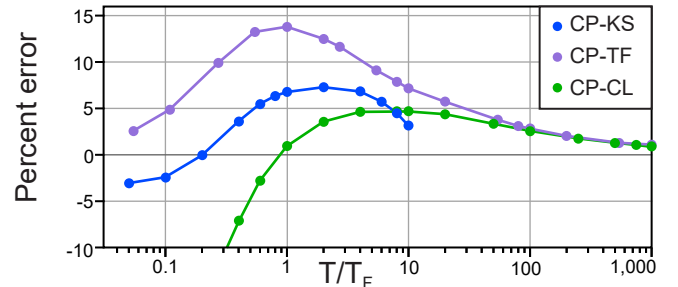


FIG. 5. Percentage error of uniform gas potential XC free energy per electron for the CP-DFT calculations within KS (blue), TF (purple), and classical (green) approximations relative to the parameterization of Groth et al. [17]. See Fig. 1 (c) for additional context.

Lastly, we mention a connection with factorization schemes in the ground state. Eq. 9 can be used to find a differential equation for  $\tilde{\Psi}_{\mathbf{r}}^{\lambda}(2\dots N)$ . But this is *not* an eigenvalue equation that you solve with given boundary conditions. Such conditional wavefunctions are not always the lowest eigenstate if one treats this as an eigenvalue problem [49]. Moreover, the potential experienced by  $\tilde{\Psi}_{\mathbf{r}}^{\lambda}(2\dots N)$  depends on all  $N-1$  coordinates, so it is not amenable to the standard KS treatment. Thus this seems an unlikely route for deriving other exact properties.

In conclusion, CP-DFT calculations provide a useful alternative to standard KS-DFT. While more expensive, they are highly parallelizable and in important cases, can succeed where KS-DFT often fails. Most importantly, such calculations bypass the need to approximate the XC functional and its potential in difficult cases, such as bond breaking. Our CP potential approximation becomes exact in many limits. It may be exact even for strictly correlated electrons, where

$$\tilde{n}_{\mathbf{r}}^{\lambda}(\mathbf{r}') \rightarrow \sum_{j=1}^{N-1} \delta^{(3)}(\mathbf{r}' - \mathbf{f}_j(\mathbf{r})), \quad (23)$$

and  $\mathbf{f}_j(\mathbf{r})$  is a co-motion function [50, 51]. Several longer works will follow.

R.J.M. supported by University of California President's Postdoctoral Fellowship, K.B. and D.P. by DOE DE-FG02-08ER46496, R.P. and S.R.W by DOE DE-SC0008696, and R.E. by Leverhulme Trust EM 2020-029/4. K.B. thanks John Perdew for suggesting a variation on this in 1993.

\* kieron@uci.edu

- [1] K. Burke, J. Chem. Phys. **136** (2012).
- [2] R. J. Bartlett and M. Musial, Rev. Mod. Phys. **79**, 291 (2007).
- [3] J. Čížek, The Journal of Chemical Physics **45**, 4256 (1966).
- [4] J. B. Anderson, The Journal of Chemical Physics **65**, 4121 (1976).

[5] B. M. Austin, D. Y. Zubarev, and W. A. Lester, *Chemical Reviews* **112**, 263 (2012).

[6] W. Kohn and L. J. Sham, *Phys. Rev.* **140**, A1133 (1965).

[7] S. Lehtola, C. Steigemann, M. J. Oliveira, and M. A. Marques, *SoftwareX* **7**, 1 (2018).

[8] N. D. Mermin, *Phys. Rev.* **137**, A: 1441 (1965).

[9] F. Graziani, M. P. Desjarlais, R. Redmer, and S. B. Trickey, eds., *Frontiers and Challenges in Warm Dense Matter*, Lecture Notes in Computational Science and Engineering, Vol. 96 (Springer International Publishing, 2014).

[10] M. Bonitz, T. Dornheim, Z. A. Moldabekov, S. Zhang, P. Hamann, H. Kahlert, A. Filinov, K. Ramakrishna, and J. Vorberger, *Physics of Plasmas* **27**, 042710 (2020), <https://doi.org/10.1063/1.5143225>.

[11] R. M. Dreizler and E. K. U. Gross, *Density Functional Theory: An Approach to the Quantum Many-Body Problem* (Springer-Verlag, Berlin, 1990).

[12] M.-C. Kim, E. Sim, and K. Burke, *J. Chem. Phys.* **134**, 171103 (2011).

[13] J. P. Perdew, K. Burke, and M. Ernzerhof, *Phys. Rev. Lett.* **77**, 3865 (1996), *ibid.* **78**, 1396(E) (1997).

[14] J. K. Percus, *Phys. Rev. Lett.* **8**, 462 (1962).

[15] K. Burke, J. Perdew, and D. Langreth, *Phys. Rev. Lett.* **73**, 1283 (1994).

[16] J. P. Perdew and Y. Wang, *Phys. Rev. B* **45**, 13244 (1992).

[17] S. Groth, T. Dornheim, T. Sjostrom, F. D. Malone, W. M. C. Foulkes, and M. Bonitz, *Phys. Rev. Lett.* **119**, 135001 (2017).

[18] D. Langreth and J. Perdew, *Solid State Commun.* **17**, 1425 (1975).

[19] M. Levy, *Proceedings of the National Academy of Sciences of the United States of America* **76**, 6062 (1979).

[20] E. H. Lieb, *Int. J. Quantum Chem.* **24**, 243 (1983).

[21] K. Burke, J. P. Perdew, and M. Ernzerhof, *The Journal of Chemical Physics* **109**, 3760 (1998).

[22] M. Levy, J. P. Perdew, and V. Sahni, *Phys. Rev. A* **30**, 2745 (1984).

[23] J. P. Perdew and A. Zunger, *Phys. Rev. B* **23**, 5048 (1981).

[24] S. H. Vosko, L. Wilk, and M. Nusair, *Can. J. Phys.* **58**, 1200 (1980).

[25] J. P. Perdew and Y. Wang, *Phys. Rev. B* **46**, 12947 (1992).

[26] S. R. White, *The Journal of Chemical Physics* **147**, 244102 (2017).

[27] S. R. White and E. M. Stoudenmire, *Phys. Rev. B* **99**, 081110 (2019).

[28] S. R. White, *Phys. Rev. B* **48**, 10345 (1993).

[29] C. Lanczos, *Journal of Research of the National Bureau of Standards* **45**, 255 (1950).

[30] H. Cox, A. L. Baskerville, V. Syrjanen, and M. Melgaard, *Advances in Quantum Chemistry* (2020).

[31] W. Heitler and F. London, *Z. Physik* **44**, 455 (1927).

[32] J. P. Perdew, A. Savin, and K. Burke, *Phys. Rev. A* **51**, 4531 (1995).

[33] S. Kais, D. Herschbach, N. Handy, C. Murray, and G. Laming, *The Journal of chemical physics* **99**, 417 (1993).

[34] M.-C. Kim, E. Sim, and K. Burke, *Phys. Rev. Lett.* **111**, 073003 (2013).

[35] T. Dornheim, S. Groth, and M. Bonitz, *Physics Reports* **744**, 1 (2018).

[36] S. Pittalis, C. R. Proetto, A. Floris, A. Sanna, C. Bersier, K. Burke, and E. K. U. Gross, *Phys. Rev. Lett.* **107**, 163001 (2011).

[37] J. C. Smith, A. Pribram-Jones, and K. Burke, *Phys. Rev. B* **93**, 245131 (2016).

[38] L. H. Thomas, *Math. Proc. Camb. Phil. Soc.* **23**, 542 (1927).

[39] E. Fermi, *Zeitschrift für Physik A Hadrons and Nuclei* **48**, 73 (1928).

[40] R. P. Feynman, N. Metropolis, and E. Teller, *Phys. Rev.* **75**, 1561 (1949).

[41] J. Larsen, *Foundations of High-Energy-Density Physics: Physical Processes of Matter at Extreme Conditions* (Cambridge University Press, 2017).

[42] F. Perrot, *Phys. Rev. A* **20**, 586 (1979).

[43] J.-P. Hansen and I. R. McDonald, eds., *Theory of Simple Liquids*, fourth edition ed. (Academic Press, Oxford, 2013).

[44] R. Evans, *Advances in Physics* **28**, 143 (1979).

[45] N. W. Ashcroft and N. D. Mermin, *Solid State Physics*, edited by D. G. Crane (Saunders College Publishing, 1976) p. 826.

[46] J. Chihara, *Journal of Physics: Condensed Matter* **3**, 8715 (1991).

[47] A. J. Archer, B. Chacko, and R. Evans, *The Journal of Chemical Physics* **147**, 034501 (2017), <https://doi.org/10.1063/1.4993175>.

[48] J. A. Anta and A. A. Louis, *Phys. Rev. B* **61**, 11400 (2000).

[49] S. K. Min, A. Abedi, K. S. Kim, and E. K. U. Gross, *Phys. Rev. Lett.* **113**, 263004 (2014).

[50] P. Gori-Giorgi, M. Seidl, and G. Vignale, *Phys. Rev. Lett.* **103**, 166402 (2009).

[51] S. Giarrusso, S. Vuckovic, and P. Gori-Giorgi, *Journal of Chemical Theory and Computation* **14**, 4151 (2018), pMID: 29906106, <https://doi.org/10.1021/acs.jctc.8b00386>.